Supplementary Information – Article

A doublet state palladium(I) N-heterocyclic carbene complex as a dopant and stabilizer for improved photostability in organic solar cells

Aliah El Astal-Quirós [1,2,3], Valentina Carrarini [1], Francesca Zarotti [1], Atiq Ur Rahman [1], Agustí Lledós [4], Cristina G. Yebra [3], Ernesto de Jesús [3] and Andrea Reale [1]*

[1] CHOSE (Centre for Hybrid and Organic Solar Energy) and Department of Electronic Engineering, University Rome Tor Vergata, Via del Politecnico 1, 00133 Rome, Italy; aliah1995@hotmail.com (A.E.A.-Q.); valentina.carrarini@gmail.com (V.C.) ; francesca.zarotti@uniroma2.it (F.Z.); atiq986@yahoo.com (A.U.R.)

[2] DGTCSI-ISCTI (Direzione Generale per le Tecnologie delle Comunicazioni e la Sicurezza Informatica-Istituto Superiore delle Comunicazioni e delle Tecnologie Dell'informazione), Ministero dell'Impresa e del Made in Italy (MIMIt), Viale America, 201, 00144 Rome, Italy

[3] Departamento de Química Orgánica y Química Inorgánica, Instituto de Investigación Química "Andrés M. del Rio", Universidad de Alcalá, Campus Universitario, E28805 Alcalá de Henares, Madrid, Spain; cgarcia.yebra@uah.es (C.G.Y.); ernesto.dejesus@uah.es (E.D.J)

[4] Department de Química, Universitat Autònoma de Barcelona, 08193 Bellaterra Barcelona, Spain; agusti.lledos@uab.cat (A.L.)

* Correspondence: reale@uniroma2.it

Table of contents

1. Synthesis of palladium complexes

1.1 General procedures

Synthetic techniques. All operations were performed under an argon atmosphere using Schlenk or dry-box techniques. Tris(dibenzylideneacetone)dipalladium ($Pd_2(dba)_3$), [1,2] 1,3-bis(2,6-diisopropylphenyl)imidazolium chloride (IPr·HCl), [3,4] and ferrocenium hexafluoridophosphate ($[FeCp_2][PF_6]$) [5] were prepared according to literature procedures. Unless otherwise stated, all other reagents were obtained from commercial sources and used as received. 1,2-Difluorobenzene (Fluorochem, 98%) was distillated under argon and deoxygenated prior to use. Other solvents (HPLC grade) were purified by flash column chromatography and collected under argon, using a MBraun MB SPS solvent purification device.

EPR spectroscopy. CW-EPR spectra were performed in a Bruker EMX spectrometer at the C. A. I. de Resonancia Magnética Nuclear y de Espín Electrónico of the Universidad Complutense de Madrid. EPR data were obtained using a 20 mW microwave power in a HSW-10432 cavity at 9.46 GHz, with 4 G field modulation at 100 kHz. For measurements in frozen solutions, the complex was dissolved in 2 mL of the appropriate solvent (molar concentration of 10^{-3} M) and the solution was quickly frozen with liquid nitrogen. EPR spectra were simulated using the software EasySpin [6,7] in combination with the SimLabel graphical user interface [8].

Mass spectrometry. Mass spectra were recorded at the Analytical Services of the Universidad de Alcalá using an Agilent 6210-TOF LC/MS mass spectrometer with an ESI ion source. After dissolution in the appropriate solvent, the samples were directly pumped into the mass spectrometer and analyzed without additives.

Elemental analyses. The Analytical Services of the Universidad de Alcalá performed the C, H, and N analyses using a LECO CHNS-932 microanalyzer.

Safety Statement. The procedures outlined in this report have been described so that they can be safely reproduced by personnel trained in the common hazards associated with chemical synthesis (use of flammable solvents, handling of cryogenic liquids, use of vacuum lines, etc.). All volatile substances should be handled in a fume hood. No uncommon hazards are noted following the procedures described in this work, provided they are performed by trained personnel on the scale reported herein.

2. Synthesis and characterization of bis[1,3-bis-(2,6-diisopropylphenyl)-4,5-dichloroimidazol-2-ylidene]palladium(0), [Pd(IPr^{Cl})$_2$] (1)

Synthesis. Under an inert atmosphere, a solution of 1,3-bis(2,6-diisopropylphenyl)-4,5-dichloroimidazol-2-ylidene [9] (IPr^{Cl} ; 3.15 g, 9.30 mmol) in DMF (10 mL) was added (cannulated) to a second solution of [Pd$_2$(dba)$_3$] [10][1] (2.67 g, 4.65 mmol) in DMF (20 mL). After 30 h of reaction, the initial brown mixture changed to produce a bright orange precipitate which was isolated by filtration. This precipitate was extracted with hexane (3 x 30 mL) and the filtrates were dried under vacuum to give an orange powder (3.19 g, 77.4 %).

Characterization data. Anal. Calcd. (%) for $C_{54}H_{68}Cl_4N_4Pd$: C, 63,50; H, 6,71; N, 5,49. Found: C, 63.50; H, 6.68; N, 5.57. ^{1}H NMR (300 MHz, C_6D_6, 7.16 ppm): δ 7.26 (t, J = 7.5 Hz, 4H, Ar-*p*-CH), 7.04 (d, J = 7.5 Hz, 8H, Ar-*m*-CH), 2.79 (sept, J = 6.0, 8H, CH(CH$_3$)$_2$) 1.17 (d, J = 6.0, 24H, CH$_3$), 1.15 (d, J = 6.0, 24H, CH$_3$).

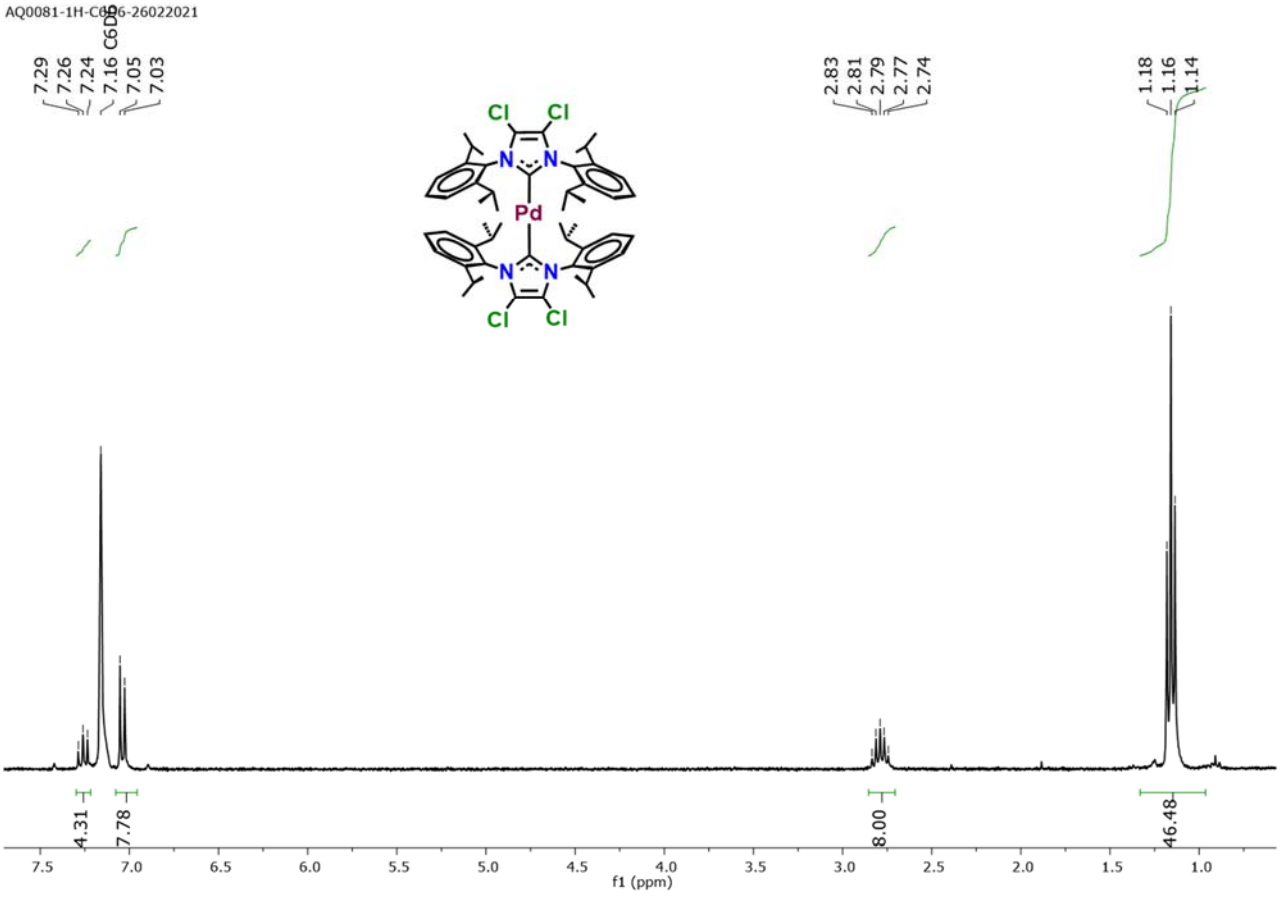

Figure S1. ^{1}H NMR spectrum (300 MHz) for [Pd(IPr^{Cl})$_2$] in benzene-*d*$_6$

3. Synthesis and characterization of bis-[1,3-bis-(2,6-diisopropylphenyl)-4,5-dichloroimidazol-2-ylidene]palladium(I) hexafluoridophosphate, [Pd(IPr^{Cl})$_2$][PF$_6$] (2)

Synthesis. Complex **2** was prepared according to synthetic methodology described by us [11]. [Pd(IPr^{Cl})$_2$] (1.589 g, 1.56 mmol) was reacted with one equivalent of ferrocenium hexafluorophosphate (0.532 g, 1.56 mmol, 97%) in 1,2-difluorobenzene (20 mL). The mixture was stirred for 2h at room temperature and then was filtered and concentered under reduced pressure. Hexane was added (60 mL) to precipitate a yellow-green complex which was isolated by filtration. (1.183 g, 65.0 %). Complex **2** is stable for an indefinite period in air in the solid state and can be handled without special precautions. The complex is stable for at least several days in solution at room temperature under inert atmosphere but decomposes more rapidly under dioxygen.

Characterization data. Anal. Calcd. (%) for $C_{54}H_{68}Cl_4F_6N_4PPd$: C, 55.61; H, 5.88; N, 4.80. Found: C, 55.38; H, 5.83; N, 5.09. ESI-MS (positive ion, acetone) : *m*/*z* 1018.48 [calcd. for **2**-$PF_6]^+$, $C_{54}H_{68}Cl_4N_4Pd^+$ 1018.32) 100%.

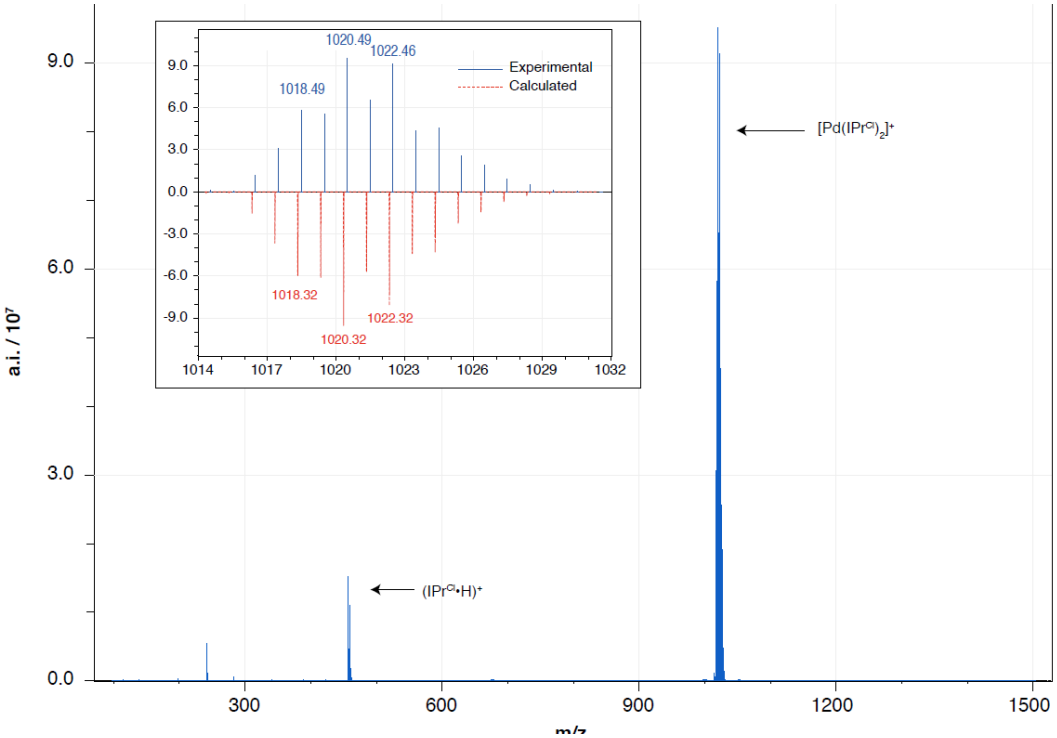

Figure S2. Mass spectrum of [Pd(I)IPr$^{Cl}_2$][PF_6] (2). ESI-TOF(+) mass spectrum of 2 in acetone. The inset shows an enlarged view of the experimental (blue lines and digits) and calculated peaks (red lines and digits) corresponding to the [Pd(IPr^{Cl})$_2$]$^+$ molecular ion.

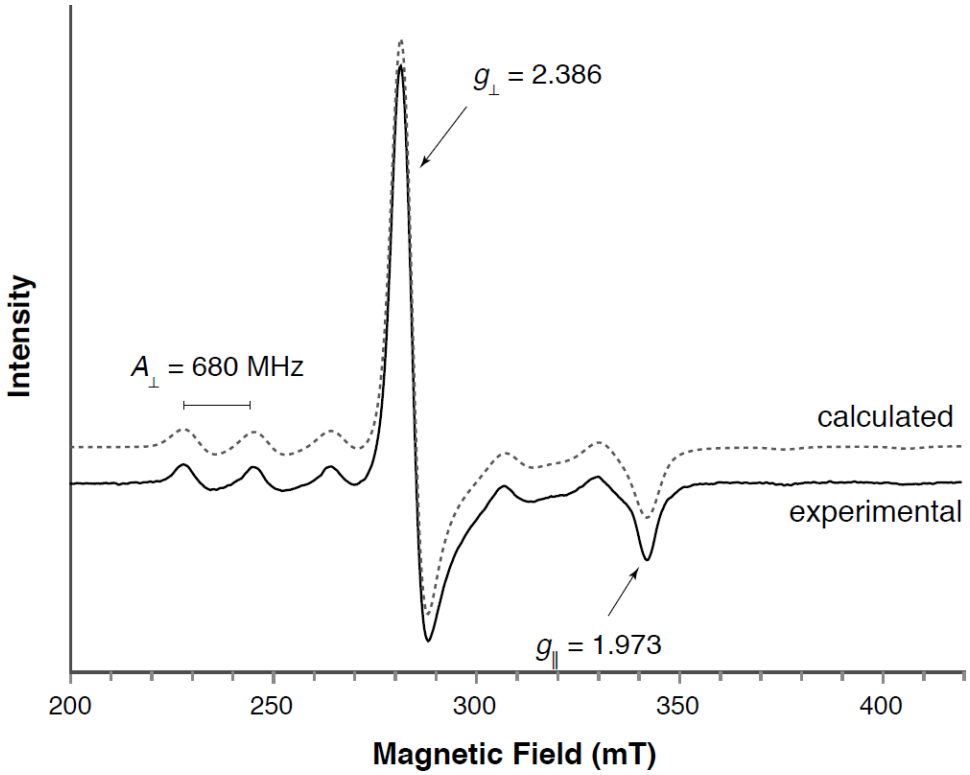

Figure S3. EPR spectrum of [Pd^{I}IPr$^{Cl}_2$][PF$_6$] (2)

2. DFT calculations of the energies of the highest occupied and lowest unoccupied molecular orbitals (MOs) of $[Pd(IPr^{Cl})_2][PF_6]$ (2)

Computational Details. Unrestricted Density Functional calculations (UDFT) were carried out using the Gaussian 16 suite of programs [12], to optimize the geometry of the cation radical $[Pd(IPr^{Cl})_2]^{+\cdot}$ in the doublet spin state. The hybrid meta-GGA TPSSh functional [13], supplemented with the Grimme's D3 correction to account for dispersion effects,[14] was employed. Optimizations were carried out in solution (solvent = 2-hexanone, ε = 14.136) using the SMD continuum model [15] with basis set 1 (BS1). In BS1 the Pd atoms is described by means of an effective core potential SDD for the inner electrons and its associated double-ζ basis set for the outer ones [16], complemented with a set of f-polarization functions [17]. The triple-ξ 6-311G(d,p) basis set is used for the H, C, N and Cl atoms [18]. The nature of minimum of the optimized structure has been verified by a frequency calculation.

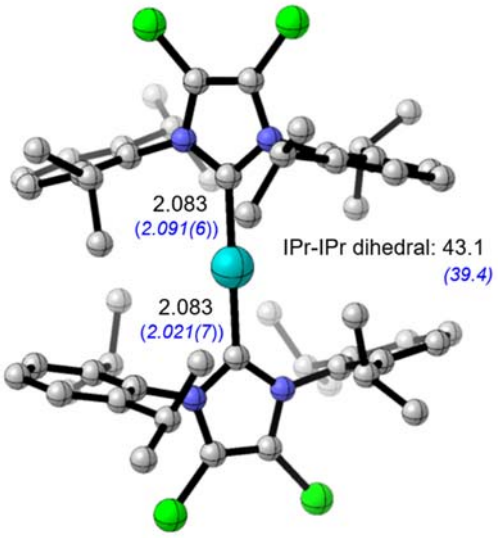

Figure S4. DFT (UTPPSh-D3/BS1) optimized structure of $[Pd(IPr^{Cl})_2]^{+\cdot}$ Geometrical parameters are very similar to those of the X-ray structure of $[PdI(IPr)_2]PF_6$ Errore. Il segnalibro non è definito. **(in blue).**

Spin density distribution. The metalloradical nature of the complex can be appreciated in the spin density distribution, obtained as the difference between the α electron density and the β electron density. The unpaired electron mainly resides in the palladium center (Figure S5). By comparing Figures S5 and S6 it can be seen that the spin density distribution maps the tridimensional shape of the single occupied molecular orbital (SOMO).

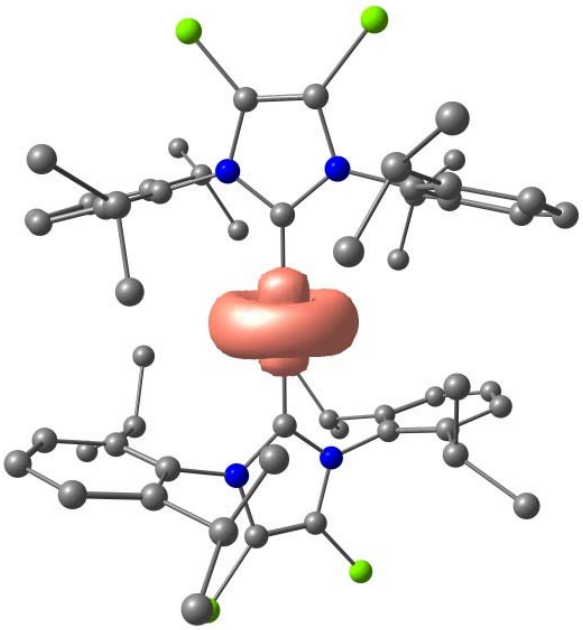

Figure S5. DFT computed spin density distribution for of $[Pd(IPr^{Cl})_2]^{+\cdot}$. Isosurface plot at 0.004. H atoms omitted.

Plot of HOMO and LUMO spin-orbitals of $[Pd(IPr^{Cl})_2]^{+\cdot}$

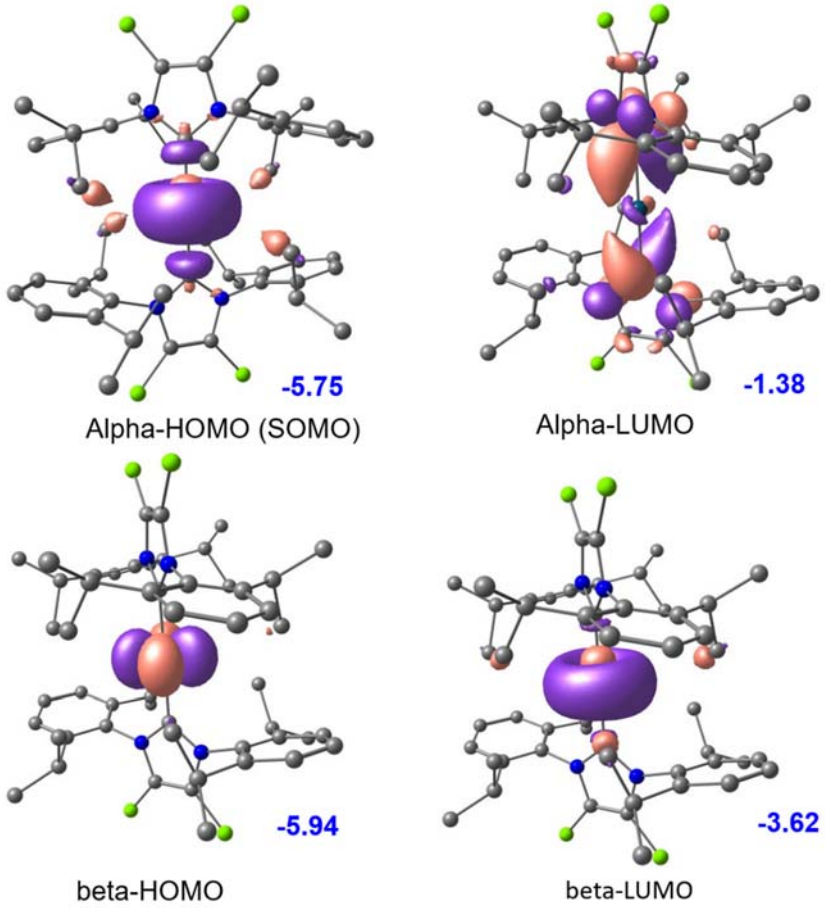

Figure S6. Highest occupied and lowest unoccupied α and β Molecular Orbitals of $[Pd(IPr^{Cl})_2]^{+\cdot}$. Isosurface plot at 0.04. H atoms omitted. In blue, orbital energies (in eV).

Cartesian coordinates and energy (in hartrees) of the optimized structure of $[Pd(IPr^{Cl})_2]^{+\cdot}$

E(UTPSSh) = -4287.305683 hartrees

6	-2.081864000	0.030650000	0.001996000
6	-4.273411000	-0.555391000	-0.233952000
6	-4.244858000	0.707788000	0.257943000
6	-2.608133000	-2.273191000	-0.868379000
6	-2.501011000	2.354124000	0.873369000
6	-2.647333000	-2.504227000	-2.255139000
6	-2.526613000	2.594274000	2.259036000
6	-2.403654000	-3.812009000	-2.683319000
6	-2.223201000	3.891885000	2.679752000
6	-2.135608000	-4.826369000	-1.763908000
6	-1.911757000	4.888418000	1.754398000
6	-2.120396000	-4.563443000	-0.397371000
6	-1.910664000	4.617534000	0.389396000
6	-2.386822000	-3.275667000	0.085882000
6	-2.234965000	3.340227000	-0.086315000
6	-2.444243000	-2.982928000	1.576492000
6	-2.302722000	3.041681000	-1.575033000
6	-1.025199000	-2.796381000	2.129217000
6	-0.888068000	2.829911000	-2.129871000
6	-3.199617000	-4.068714000	2.357661000
6	-3.042137000	4.137317000	-2.357788000
6	-2.932936000	-1.368547000	-3.227623000
6	-2.858088000	1.477468000	3.238471000
6	-1.644030000	-0.579505000	-3.519051000
6	-1.601404000	0.638341000	3.529994000
6	-3.591743000	-1.834833000	-4.531216000
6	-3.492114000	1.978245000	4.541458000
6	3.576633000	1.819097000	-4.537014000
6	3.514049000	-1.988126000	4.534343000
6	1.630944000	0.566088000	-3.518016000
6	1.622993000	-0.642687000	3.529251000
6	2.454628000	2.993609000	1.567415000
6	2.284403000	-3.030851000	-1.579972000
6	3.202987000	4.087956000	2.342983000
6	3.027891000	-4.116564000	-2.372744000
6	1.039038000	2.796663000	2.125932000
6	0.862774000	-2.832408000	-2.120916000
6	2.083131000	-0.029857000	0.003295000
6	4.273102000	0.558710000	-0.240648000
6	4.247830000	-0.705274000	0.249518000
6	2.603538000	2.272630000	-0.874306000
6	2.507233000	-2.353787000	0.868839000
6	2.388248000	3.280429000	0.075949000
6	2.231925000	-3.335759000	-0.092234000
6	2.118013000	4.565276000	-0.412481000
6	1.910710000	-4.614775000	0.381005000
6	2.122945000	4.820428000	-1.780703000
6	1.922206000	-4.890625000	1.744969000
6	2.386393000	3.801458000	-2.696149000
6	2.240059000	-3.897290000	2.671689000
6	2.634849000	2.496261000	-2.262403000
6	2.541260000	-2.598341000	2.253418000

6	2.919571000	1.356979000	-3.230986000
6	2.877573000	-1.483956000	3.234006000
7	-2.949716000	-0.953236000	-0.391798000
7	-2.904444000	1.049550000	0.403526000
7	2.948548000	0.955602000	-0.392250000
7	2.908290000	-1.048107000	0.400533000
46	0.000533000	-0.000064000	-0.001949000
17	5.599981000	1.557322000	-0.620558000
17	5.532797000	-1.759077000	0.623564000
17	-5.602859000	-1.552800000	-0.607800000
17	-5.527617000	1.761535000	0.639997000

3. SEM data

3.1 Spectra

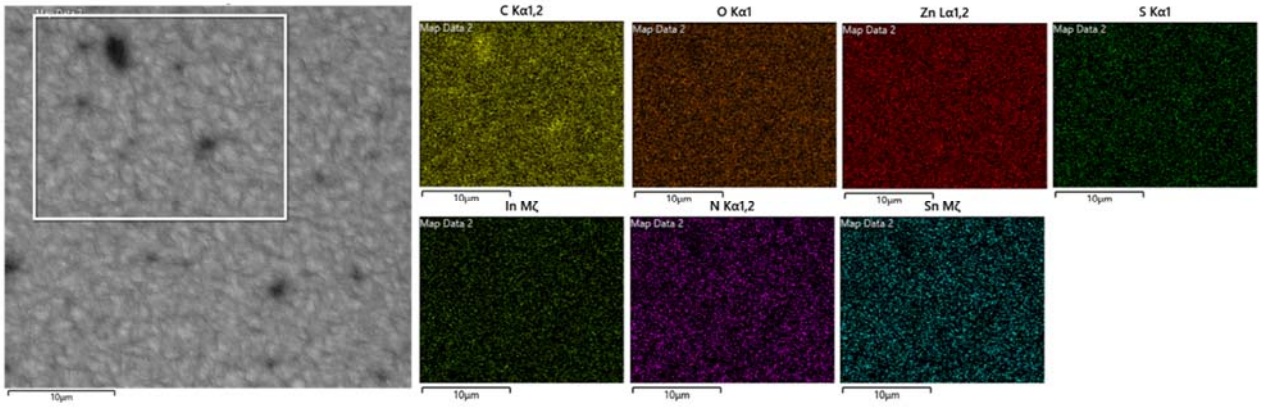

Figure S7- EDS map of the Reference device without Pd complex. Measurement was performed at 5 keV.

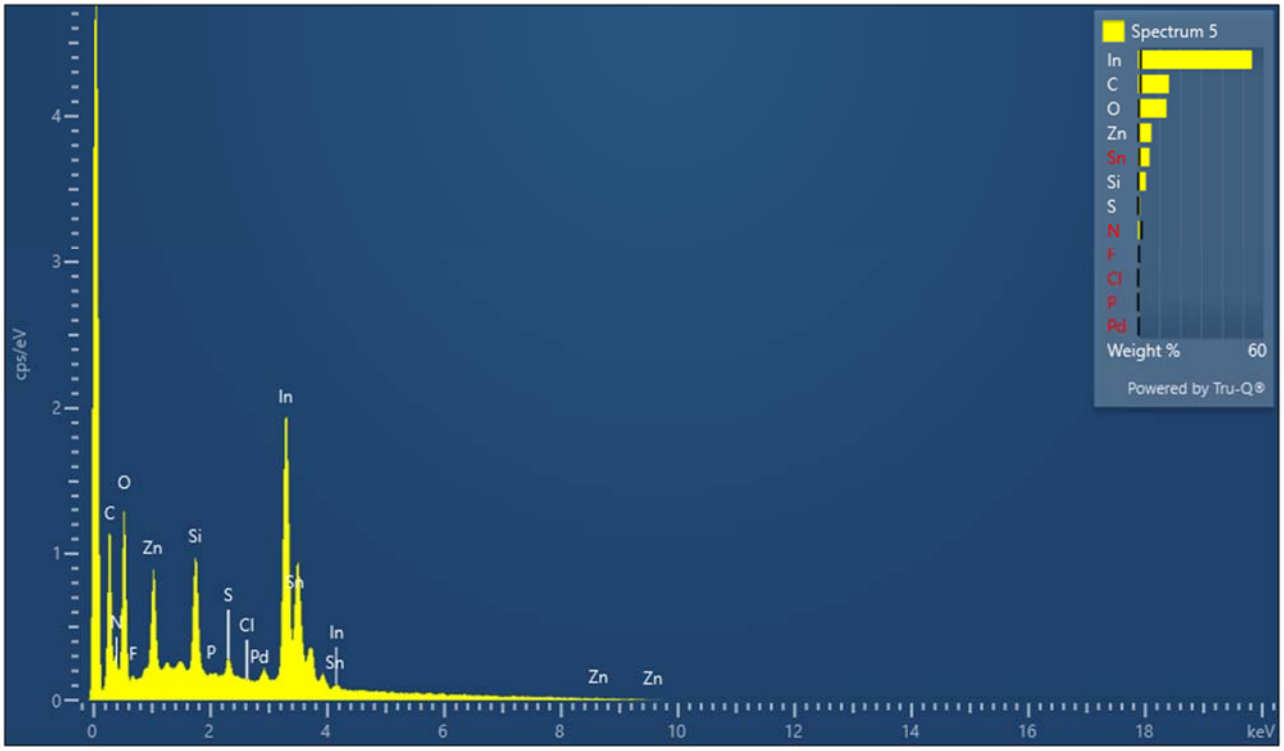

Figure S8- EDS spectrum of the device with 0.1 wt% of Pd complex. Pd complex elements are detected. Pd element can be detected around 2.8 eV. Measurement was performed at 10 keV. (Elements displayed in red signify that the peak used for quantification is only just above statistical noise and less than 10σ)

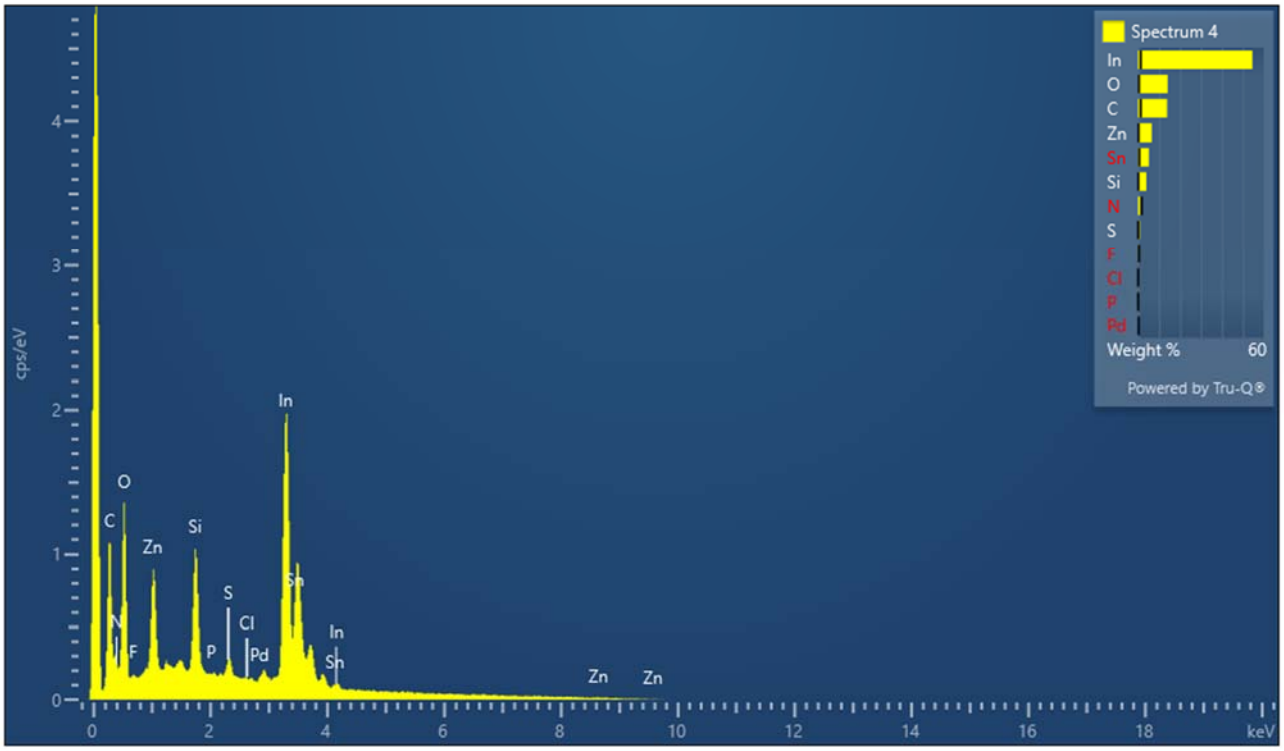

Figure S9- EDS spectrum of the device with 1.0 wt% of Pd complex. Pd complex elements are detected. Pd element can be detected around 2.8 eV. Measurement was performed at 10 keV. (Elements displayed in red signify that the peak used for quantification is only just above statistical noise and less than 10σ)

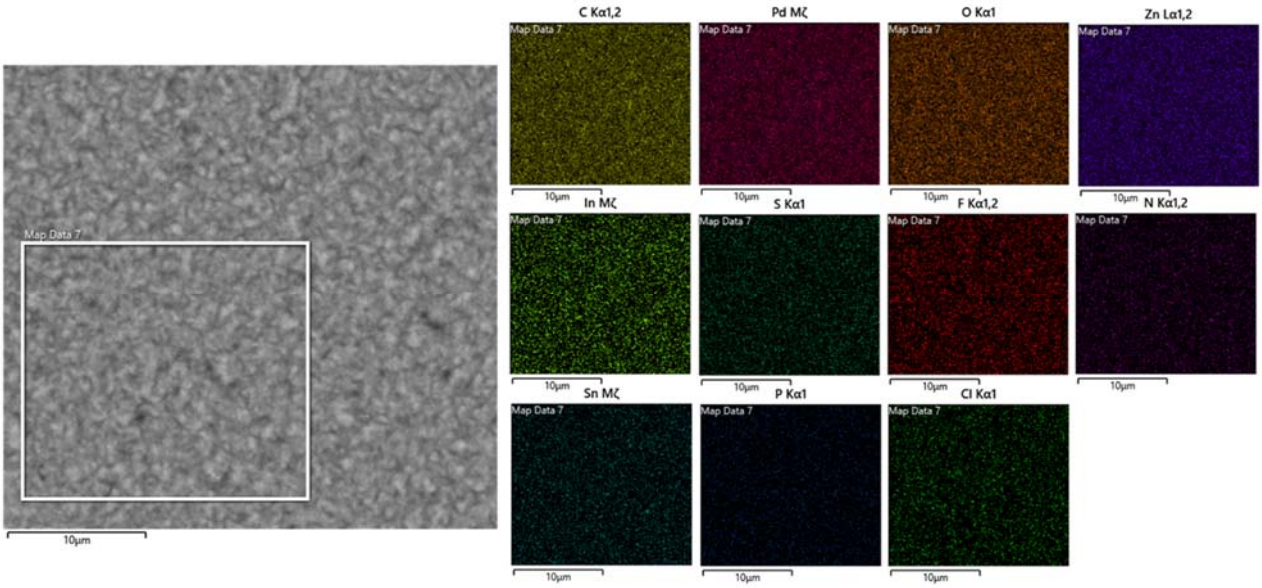

Figure S10- EDS map of the device with 6.0 wt% of Pd complex. Pd complex elements are detected. Pd element can be detected around 2.8 eV. Measurement was performed at 5 keV.

3.2. Elemental quantities of the different devices

Table S1- Elemental analysis of the reference device

Element	Line Type	Apparent Concentration	Atomic %
C	K series	0.92	56.72
N	K series	0.10	1.12
O	K series	1.21	24.32
Si	K series	0.00	0.00
S	K series	0.15	2.67
Zn	L series	0.41	5.78
In	L series	1.09	8.46
Sn	L series	0.11	0.94
Total:			100.00

Table S2- Elemental analysis of the 0.1 wt% of additive device

Element	Line Type	Apparent Concentration	Atomic %
C	K series	0.99	57.45
N	K series	0.20	2.19
O	K series	1.16	22.44
F	K series	0.10	0.95
Si	K series	0.00	0.08
P	K series	0.02	0.19
S	K series	0.12	2.05

Cl	K series	0.02	0.34
Zn	L series	0.36	4.98
Pd	L series	0.04	0.37
In	L series	1.14	8.57
Sn	L series	0.05	0.41
Total:			100.00

Table S3- Elemental analysis of the 1.0 wt% of additive device

Element	Line Type	Apparent Concentration	Atomic %
C	K series	0.98	57.04
N	K series	0.20	2.15
O	K series	1.22	22.88
F	K series	0.10	0.88
Si	K series	0.01	0.20
P	K series	0.01	0.16
S	K series	0.15	2.53
Cl	K series	0.01	0.08
Zn	L series	0.41	5.47
Pd	L series	0.04	0.30
In	L series	1.04	7.63
Sn	L series	0.08	0.67
Total:			100.00

Table S4- Elemental analysis of the 6.0 wt% of additive device

Element	Line Type	Apparent Concentration	Atomic %
C	K series	1.05	61.35
N	K series	0.00	0.00
O	K series	1.19	22.42
F	K series	0.00	0.00
P	K series	0.00	0.00
S	K series	0.13	2.20
Cl	K series	0.02	0.33
Zn	L series	0.41	5.55
Pd	L series	0.05	0.46
In	L series	0.83	6.24
Sn	L series	0.18	1.46
Total:			100.00

4. References

1. Walter, R.; Meyer, H.; Voss, S. Palladium(0)-dibenzylidene acetone complexes, US Patent, 2010/0167408A1, Jul 1, **2010**.

2. Kapdi, A. R.; Whitwood, A. C.; Williamson, D. C.; Lynam, J. M.; Burns, M. J.; Williams, T. J.; Reay, A. J.; Holmes, J.; Fairlamb, I. J. S. The Elusive Structure of $Pd_2(dba)_3$. Examination by Isotopic Labeling, NMR Spectroscopy, and X-ray Diffraction Analysis: Synthesis and Characterization of $Pd_2(dba\text{-}Z)_3$ Complexes. *J. Am. Chem. Soc.* **2013**, 135, 8388-8399.

3. Huang, J.; Nolan, S. P. Efficient Cross-Coupling of Aryl Chlorides with Aryl Grignard Reagents (Kumada Reaction) Mediated by a Palladium/Imidazolium Chloride System. *J. Am. Chem. Soc.* 1999, 121, 9889-9890.

4. Jafarpour, L.; Stevens, E. D.; Nolan, S. P. A sterically demanding nucleophilic carbene: 1,3-bis(2,6-diisopropylphenyl)imidazol-2-ylidene). Thermochemistry and catalytic application in olefin metathesis. *J. Organomet. Chem.* **2000**, *606*, 49-54.

5. Connelly, N. G.; Geiger, W. E. Chemical Redox Agents for Organometallic Chemistry. *Chem. Rev.* **1996**, 96, 877-910.

6. Tait, C.; Lehner, J.; Nehrkorn, J.; Krzyaniak, M.; Ho, A.; Stoll, S. EasySpin, software package for spectral simulation and analysis in EPR, version 5.2.25, **2014**, http://www.easyspin.org (accessed 11/18/2023).

7. Stoll, S.; Schweiger, A. EasySpin, a comprehensive software package for spectral simulation and analysis in EPR. *J. Magn. Reson.* **2006**, 178, 42-55.

8. Etienne, E.; Le Breton, N.; Martinho, M.; Mileo, E.; Belle, V. SimLabel: a graphical user interface to simulate continuous wave EPR spectra from site-directed spin labeling experiments. *Magn. Reson. Chem.* **2017**, 55, 714-719.

9. Arduengo III, A. J., Krafczyk, R., Schmutzler, R., Craig, H. A., Goerlich, J. R., Marshall, W. J., & Unverzagt, M. *Imidazolylidenes, imidazolinylidenes and imidazolidines. Tetrahedron*. **1999**, 55(51), 14523-14534.

10. Zalesskiy, S. S., & Ananikov, V. P. $Pd_2(dba)_3$ as a precursor of soluble metal complexes and nanoparticles: Determination of palladium active species for catalysis and synthesis. *Organometallics*, **2012**, 31(6), 2302-2309.

11. Maties G, Gómez-Sal P, Yebra CG, Andrés R, de Jesús E. Reversible Single-Electron-Transfer to Oxygen in a Stable N-Heterocyclic Carbene Palladium(I) Metalloradical. *Inorg Chem.* **2023**, 62(49), 19838-19842.

12. Gaussian 16, Revision C.01, Frisch, M. J.; Trucks, G. W.; Schlegel, H. B.; Scuseria, G. E.; Robb, M. A.; Cheeseman, J. R.; Scalmani, G.; Barone, V.; Petersson, G. A.; Nakatsuji, H.; Li, X.; Caricato, M.; Marenich, A. V.; Bloino, J.; Janesko, B. G.; Gomperts, R.; Mennucci, B.; Hratchian, H. P.; Ortiz, J. V.; Izmaylov, A. F.; Sonnenberg, J. L.; Williams-Young, D.; Ding, F.; Lipparini, F.; Egidi, F.; Goings, J.; Peng, B.; Petrone, A.; Henderson, T.; Ranasinghe, D.; Zakrzewski, V. G.; Gao, J.; Rega, N.; Zheng, G.; Liang, W.; Hada, M.; Ehara, M.; Toyota, K.; Fukuda, R.; Hasegawa, J.; Ishida, M.; Nakajima, T.; Honda, Y.; Kitao, O.; Nakai, H.; Vreven, T.; Throssell, K.; Montgomery, J. A., Jr.; Peralta, J. E.; Ogliaro, F.; Bearpark, M. J.; Heyd, J. J.; Brothers, E. N.; Kudin, K. N.; Staroverov, V. N.; Keith, T. A.; Kobayashi, R.; Normand, J.; Raghavachari, K.; Rendell, A. P.;

Burant, J. C.; Iyengar, S. S.; Tomasi, J.; Cossi, M.; Millam, J. M.; Klene, M.; Adamo, C.; Cammi, R.; Ochterski, J. W.; Martin, R. L.; Morokuma, K.; Farkas, O.; Foresman, J. B.; Fox, D. J. Gaussian, Inc., Wallingford CT, **2016**.

13. Staroverov, V. N.; Scuseria, G. E.; Tao, J.; Perdew, J. P. Comparative Assessment of a New Nonempirical Density Functional: Molecules and Hydrogen-Bonded Complexes. *J. Chem. Phys.* **2003**, *119*, 12129−12137. (b) Tao, J.; Perdew, J. P.; Staroverov, V. N.; Scuseria, G. E. Climbing the Density Functional Ladder: Nonempirical Meta−Generalized Gradient Approximation Designed for Molecules and Solids. *Phys. Rev. Lett.* 2003, 91, 146401.

14. Grimme, S.; Antony, J.; Ehrlich, S.; Krieg, H. A Consistent and Accurate Ab Initio Parametrization of Density Functional Dispersion Correction (DFT-D) for the 94 Elements H-Pu. *J. Chem. Phys.* **2010**, 132, 154104.

15. Marenich, A. V.; Cramer, C. J.; Truhlar, D. G. Universal Solvation Model Based on Solute Electron Density and on a Continuum Model of the Solvent Defined by the Bulk Dielectric Constant and Atomic Surface Tensions. *J. Phys. Chem. B* **2009**, 113, 6378−6396.

16. Andrae, D.; Haeussermann, U.; Dolg, M.; Stoll, H.; Preuss, H. Energy-Adjusted *Ab Initio* Pseudopotentials for the Second and Third Row Transition Elements. *Theor. Chim. Acta* **1990**, 77, 123−141.

17. Ehlers, A. W.; Bohme, M.; Dapprich, S.; Gobbi, A.; Hollwarth, A.; Jonas, V.; Kohler, K. F.; Stegmann, R.; Veldkamp, A.; Frenking, G. A Set of f-Polarization Functions for Pseudo-Potential Basis-Sets of the Transition-Metals Sc-Cu, Y-Ag and La-Au. *Chem. Phys. Lett.* **1993**, 208, 111−114

18. McLean, A, D.; Chandler, G. S. Contracted Gaussian-basis sets for molecular calculations. 1. 2nd row atoms, Z=11-18. *J. Chem. Phys.* **1980**, 72, 5639-5648. (b) Raghavachari, K.; Binkley, J. S.; Seeger, R.; Pople, J. A. Self-Consistent Molecular Orbital Methods. 20. Basis set for correlated wave-functions. *J. Chem. Phys.* **1980**, 72, 650-654.